Received: 3 January 2018 | Accepted: 28 February 2018

DOI: 10.1111/jace.15526

RAPID COMMUNICATION

Journal of the American Ceramic Society

A simple method of short-term mechanical reliability prediction for ceramics in reactive environments

Robert F. Cook

Materials Measurement Science Division, National Institute of Standards and Technology, Gaithersburg, Maryland

Correspondence
Robert F. Cook, Materials Measurement Science Division, National Institute of Standards and Technology, Gaithersburg, MD.
Email: robert.cook@nist.gov

Abstract

A method is demonstrated for prediction of ceramic reliability limited by fracture in reactive environments. The simplicity of the method relies on the ceramic displaying ideal indentation-strength behavior and on the applied loading leading to short-term power-law crack velocity behavior. Reactive failure strength measurements, treating flaw size as a variable and failure time as a constraint in a "pass-fail" test, enable reliability, including both intrinsic and contact flaws, to be predicted. Little to no computation is required.

KEYWORDS

cordierite, corrosion/corrosion resistance, crack velocity, cracks/cracking, strength

1 | INTRODUCTION

Recent works[1,2] have highlighted some of the factors complicating mechanical reliability predictions for ceramics in reactive environments. Such predictions are critical to the usefulness of ceramics and glasses in all applications and, typically, such reliability, or load-bearing capacity over time, is controlled by crack propagation. Hence, reliability predictions for ceramics usually include several complicating fracture phenomena: (1) Surface crack initiation and propagation from contact flaws is ubiquitous in ceramics. However, in many materials the tendency to chipping at large contacts diminishes the contact-induced residual stress field, greatly reducing the driving force for crack propagation; (2) In many materials with large microstructural elements, crack propagation leads to the formation of compressive traction zones of unbroken elements behind the crack tip. The zone greatly increases the fracture resistance or toughness with crack length; (3) In all materials in reactive environments there is a nonzero crack driving force—the threshold—at which the fracture system is in equilibrium and the crack velocity is zero. Proximity to the threshold greatly extends the lifetimes of components under very small driving forces; (4) Finally, in many materials in moderately corrosive environments, the geometry of contact flaws and their attendant cracks are altered dramatically by simple exposure to the environment, independent of any applied loading. Such corrosive effects often lead to strengthening effects on extended exposures. Factors (1)-(4) differ considerably in their temporal and spatial dependencies and hence the often-competing influences require sophisticated experiments and numerical analyses in order to make reliability predictions.[1]

Simple reliability predictions can be made, however, under simple conditions. In particular, if (1) meso-scale chipping effects, (2) micro-scale toughening effects, (3) crack-velocity threshold effects, and (4) corrosive exposure effects, are all small or absent, a simple method can be used to make ceramic reliability predictions. The first two effects (1 and 2), chipping and toughening, depend on the material. Chipping, and precursor lateral cracking, is reduced in materials with small ($\approx$12) modulus/hardness (E/H) ratios, similar to silicate glasses.[3] Toughening and the formation of traction zones is minimized in materials with small or absent microstructural features,[1] again similar to glasses. A material that meets these criteria, to be used here as an example, is a fine-grained cordierite glass-ceramic, similar to that studied earlier.[1,2,4] The second two effects (3 and 4), thresholds and corrosion, depend on the mechanical and chemical environment. Threshold effects are smaller under loading conditions that lead to crack velocities that remain far removed from zero during failure

and, hence, lead to short failure times. Short failure times also minimize corrosion effects, as do environments that are reactive but do not remove material through dissolution. The second two criteria are met here by loading the samples in water to obtain failure times of 1 hour (threshold and corrosion effects are observed in cordierite in about 10 hours[1,2]).

The method is based on the results of two prior works—one experimental[5] and one analytical.[6] In the experimental work, advantage is taken of controlled-flaw techniques to determine the strength or lifetime of a test component. In particular, Vickers indentation flaws are generated in the surfaces of components using controlled loads. Subsequent measurement of component strength under inert conditions as a function of indentation load provides inert strength degradation behavior: components with larger flaws are weaker, that can be analyzed for many factors including (1) and (2) above.[1] Alternatively, subsequent measurement of component lifetime as a function of applied stress under reactive conditions provides reliability behavior: components under larger stresses fail in shorter times, that can be analyzed for (3) and (4).[7] A difficulty in lifetime measurements, however, even using controlled flaws and avoiding threshold effects, is that experimental lifetimes can vary by many orders of magnitude, complicating experimentation and precluding simple analysis. This difficulty can be overcome by combining the two measurement methods to generate *reactive strength degradation* behavior: measurement of the applied stress necessary to cause component failure as a function of indentation load in a fixed time under reactive conditions. In analogy with inert tests, components with larger flaws require a smaller stress for reactive failure in a fixed time. Full details on the use of controlled flaws to exchange the independent and dependent variables in lifetime tests and in validation measurements using a borosilicate glass are considered elsewhere.[5]

In the analytical work, advantage is taken of a power-law approximation to crack-velocity behavior[7-11] in determination of indented component lifetimes.[6] Far from the threshold, crack velocity v as a function of crack driving force, for example, stress-intensity factor, K, can be approximated as a simple power law, that is, $v \sim K^{n'}$, where n' is a crack-velocity exponent appropriate to cracks at indentation flaws[6] ($n > n'$ is used for nonindentation cracks[8-11]). If the crack driving force in a component, derived from the combined applied stress and indentation fields, is arranged such that this approximation is met, the connection between lifetime and applied stress of a component is known (and is also a power law[6-11]). It is a simple matter to invert this connection to describe reactive strength degradation behavior and thence to generate reliability predictions. In particular, the failure stress, σ, is related to the indentation load, P, under both inert and reactive conditions by the logarithmic relationship

$$\log\sigma = A - B\log P \tag{1}$$

where A and B are material-, environment-, and indenter-dependent (σ is taken to represent strength generally; A and B are defined using dimensions $[\sigma]$ = MPa and $[P]$ = N). The goal of the current work is to predict A and B as function of lifetime, t_f. Meeting the constraint requires applied stresses to be large enough such that fracture systems are far from the threshold, and as a consequence t_f is short: reliability is thus restricted to short-term predictions ($t_f \approx$ hours). The usefulness of short-term reliability predictions is for temporary components (e.g., as part of a repair) or for expendable components (e.g., as part of an armament). This is another way of looking at reliability: Not "how long will a component survive?"[8] but "what are the limits of flaw size and stress that will allow a component to survive a specified time?".

The material used here was a cordierite ($2MgO{\cdot}2Al_2O_3{\cdot}5SiO_2$) glass-ceramic, similar, but slightly denser after sintering (0.995 ± 0.004 relative density measured by Archimedes' method) to that used in previous strength studies (0.990 ± 0.004 relative density)[1,2,4] (unless otherwise stated, all quantities and symbols reported here are given as mean ± standard deviation of experimental measurements). The initial samples were in the form of discs with diameter 31.8 mm and thickness 2.1 mm, and inert strength tests were conducted on the discs. After inert strength testing, bend bars for reactive strength testing, 25 mm × 4 mm × 2.1 mm, were sawn from the broken disc samples and edge beveled. Prior to all strength testing, samples were indented in the center of a prospective tensile test face with a four-sided Vickers diamond pyramid with P varying from 0.98 N to 296 N. All tests were conducted on the as-sintered surfaces, which had roughness of approximately 5 μm. For inert strength tests, the disc samples were mounted in a flat-on-three-ball biaxial flexure rig; the radius of the inner, upper flat was 2.5 mm and the radius of the outer, lower circle on which the samples were supported by the three balls was 13.0 mm. Samples were loaded to failure in 30-50 ms, minimizing any moisture effects on strength, and failure loads, F, recorded by piezoelectric load cell. For reactive strength tests, the bar samples were mounted in a four-point bend uniaxial flexure rig; the upper span was 10.0 mm and the lower span was 20.0 mm. Samples were statically loaded in water for 1 hour and the median failure load, F, estimated from repeat pass-fail tests using increasingly refined loads. Details are given elsewhere.[5] In all tests, failure stresses were calculated from failure loads by $\sigma = kF/d^2$, where d is the sample thickness and k is a geometry term of order unity that depends on rig and sample dimensions.[12]

For inert conditions, there is no environment dependence and (for a pyramidal indenter)[1]

$$B = 1/3 \quad \text{(inert)}. \tag{2}$$

Consequently, the product $\sigma_{max}P^{1/3}$ is invariant, where σ_{max} is the inert (and hence maximum) strength at a given value of P, and the inert strength may be written in the indentation-dominant domain as follows:

$$\sigma_{max} = \langle \sigma_{max} P^{1/3} \rangle P^{-1/3} \tag{3}$$

where $\langle\rangle$ is used here to indicate an average over indentation load. Hence,

$$A = \log\langle \sigma_{max} P^{1/3} \rangle \quad \text{(inert)}. \tag{4}$$

As may be expected under inert conditions, A depends primarily on the material toughness and secondarily on the material (E/H) ratio and the indenter geometry.[1,5] At small indentation loads, failure does not occur at the introduced indentation flaw but from intrinsic flaws in the material generated by the manufacturing process, leading to a limiting upper-bound intrinsic inert strength, σ_0. The intrinsic flaws can be defined by a characteristic contact load, P_0, using Eq. (3):

$$\sigma_0 = \langle \sigma_{max} P^{1/3} \rangle P_0^{-1/3} \tag{5}$$

The inert strength response over the complete small-to-large load domain (intrinsic-to-indentation dominated) can be modeled as a smooth-minimum function:

$$\sigma^{\alpha} = \sigma_0^{\alpha} + \sigma_{max}^{\alpha} \tag{6}$$

where $\alpha < -1$ is an empirical exponent. After substitution of Eqs. (3) and (5) into Eq. (6),

$$\sigma = \sigma_0 [1 + (P/P_0)^{-\alpha/3}]^{1/\alpha} \tag{7}$$

Under reactive conditions, the parameter B is reduced from its inert value by[5]

$$B = 1/3 - 2/3n' \quad \text{(reactive)} \tag{8}$$

The parameter A is also reduced from its invariant inert value to a time-dependent reactive value:

$$\begin{aligned} A &= \log\langle \sigma_{max} P^{1/3} \rangle - f(n') - \log t_f / n' \\ &= \log\langle \sigma_f P^B \rangle \end{aligned} \quad \text{(reactive)} \tag{9}$$

where $f(n')$ is a time-invariant function of material, environment, and indenter properties[5] and, more importantly, t_f, is the fixed exposure time under reactive conditions (similar three term relations result for nonindentation cracks[8-11]). In analogy with Eq. (3), the reactive strength, σ_f, may be written in the indentation-dominant domain as

$$\sigma_f = \langle \sigma_f P^B \rangle P^{-B} \tag{10}$$

where the product $\sigma_f P^B$ is invariant. If the intrinsic flaws are unaltered by environment such that P_0 is invariant, Eq. (10) may be used to predict the upper-bound reactive strength:

$$\sigma_{0,f} = \langle \sigma_f P^B \rangle P_0^{-B} \tag{11}$$

The reactive strength over the full load range is thus given by (similar to Eq. (7))

$$\sigma_f = \sigma_{0,f} [1 + (P/P_0)^{-\alpha B}]^{1/\alpha} \tag{12}$$

A reliability prediction is made by first performing an inert strength test to determine the parameter P_0. A reactive strength test is then performed using a reference failure time, t_f^{ref}. Fitting Eq. (1) to the reactive data gives the parameters A^{ref} and B (and thus $\sigma_{0,f}$ and n' via Eqs. (11) and (8)) and the full reactive strength response. A prediction for the reactive strength behavior at a longer time, t_f^{ref}, can then be made by recognizing that:

$$A^{pre} = A^{ref} - \frac{1}{n'} \log(t_f^{pre}/t_f^{ref}) \tag{13}$$

eliminating the initial terms in the first line of Eq. (9), predicting $\sigma_{0,pre}$ using Eq. (11), and noting that the "slope" parameter n' is invariant.

Figure 1 shows the inert strength, σ_{max}, as a function of indentation load, P, for the cordierite glass-ceramic confirming the near-ideal response (logarithmic coordinates are shown at the top and right). Each open symbol represents 5-8 inert indentation strength measurements at the load indicated. The intrinsic strengths at small indentation loads are shown as the upper hatched band, on the left of the plot. Some indentation strength measurements were repeated at large indentation loads. A best fit to the indentation inert strength data using Eqs. (1)-(4) gave $\langle \sigma_{max} P^{1/3} \rangle$ = 324 MPa $N^{1/3}$ ± 30 MPa $N^{1/3}$. The intrinsic inert strength was σ_0 = 266 MPa ± 49 MPa, giving a characteristic intrinsic contact load of P_0 = 1.81 N ± 1.10 N, using Eq. (5). The upper solid line in Figure 1 is the full fit, Eq. (7) using $\alpha = -6$, to the inert strength data; the intrinsic and indentation asymptotes are evident on the left and right of the plot, respectively. The upper shaded band in Figure 1 shows one standard deviation uncertainty for the model prediction, Eq. (6), of the inert strength (the bounds on the band were determined using the quoted uncertainty bounds in $\langle \sigma_{max} P^{1/3} \rangle$ and σ_0).

Figure 1 also shows the reactive strength, σ_f, as a function of P. In this case, each filled symbol represents the median indentation reactive-failure strength, from about 12 1-hour tests, at the load indicated and the bars represent the 17 and 83 strength percentiles (enclosing 66% of the

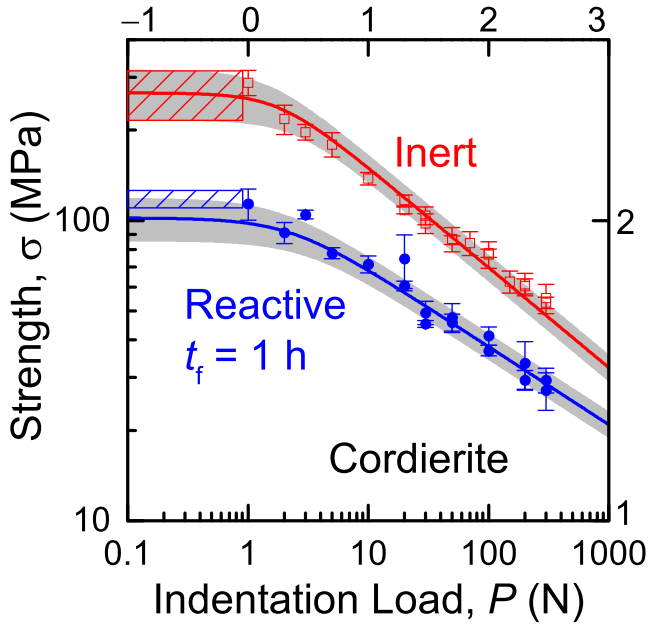

FIGURE 1 Plot of inert and reactive strengths as a function of Vickers indentation load for cordierite glass-ceramic. The symbols are experimental measurements and the solid lines are best fits assuming ideal indentation behavior and power-law crack velocity behavior. The hatched bands indicate intrinsic strengths. The shaded bands indicate fit uncertainties [Color figure can be viewed at wileyonlinelibrary.com]

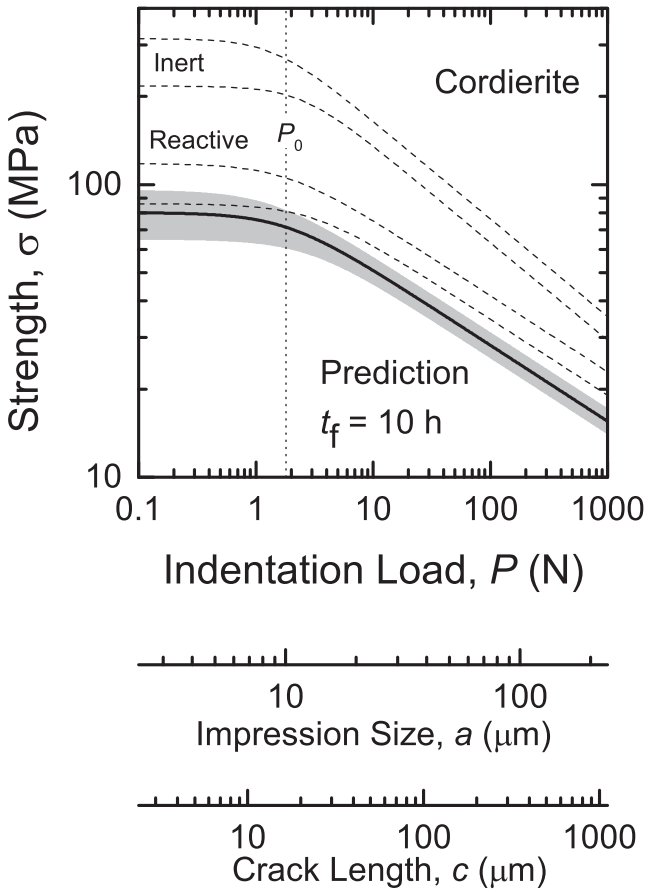

FIGURE 2 Reliability prediction plot as strength vs indentation load map for cordierite glass-ceramic, based on the measurements of Figure 1. The solid line and shaded band indicate the mean and uncertainty limits of the 10 hours failure time prediction. The dashed lines indicate the uncertainty bounds of the inert and reactive strength measurements. Alternative flaw size parameters based on the indentation load are shown

measurements, somewhat analogous to standard deviation limits, permitting an assessment of the uncertainty in the median strength). The reactive intrinsic strengths are shown as the lower hatched band and some measurements were repeated at large indentation loads. The best fit to the reactive strength data using Eq. (1) gave $A^{ref} = 2.10 \pm 0.04$ and $B = 0.260 \pm 0.025$ and thus, from Eq. (8), $n' = 9.1 \pm 0.9$, and, from Eqs. (9)-(11), the predicted upper-bound reactive strength, dominated by intrinsic flaws, was $\sigma_{0,f} = 102 \pm 16$ MPa (*cf.* measured 117 ± 9 MPa). The lower solid line in Figure 1 is the full fit to the reactive strength data using Eq. (12) and the above parameters; the asymptotes are evident as is the correct prediction of the intrinsic strength. The lower shaded band shows one standard deviation uncertainty for the model prediction of the reactive strength (replacing inert quantities in Eq. (6) using the measured reactive strength parameter A^{ref}, the predicted reactive strength limit $\sigma_{0,f}$, and their quoted uncertainty bounds).

Figure 2 shows a reliability prediction of the reactive strength, σ_f, as a function of indentation load, P, for failure time of $t_f = 10$ hours, using Eqs. (12) and (13). The solid line and shaded band show the mean and uncertainty of the 10-hour prediction. The dashed lines show the uncertainties for the best fits to the inert and 1-hour reactive strength measurements (all uncertainty bounds calculated from uncertainty bounds in A and σ_0 parameters). The vertical dotted line indicates the characteristic contact load, P_0. Two sets of axes at the bottom of Figure 2 indicate the scale of the flaws controlling the reliability: One set of axes gives the contact impression size, a, and the other gives the crack length, c. These axes are related to the indentation load by $a = (P/2 > H)^{1/2}$ and $c = (P/\langle P/c^{3/2}\rangle)^{2/3}$, where $\langle H\rangle = 9.0$ GPa $\pm$ 0.5 GPa is the hardness and $\langle P/c^{3/2}\rangle = 27.0$ MPa $m^{1/2} \pm 4.5$ MPa $m^{1/2}$ is an indentation crack-length parameter, both observed to be load-invariant here as previously[4] and hence averaged over the indentation load domain.

2 | CONCLUSIONS

Figure 2 represents an extremely powerful reliability prediction method, based on a simple pass-fail experiment and a simple, linear analysis. At its simplest, Figure 2 can be treated as a map: points to the lower left below the line (small applied stresses, small flaws) represent conditions in

which a component will survive the stated time and points to the upper right (large stresses, large flaws) represent conditions in which a component will fail. The uncertainty shown by the shaded band provides a measure of "how close to the edge" a component might be, with the recognition that the applied stress or flaws could be generated in manufacturing or in service. The scale of the flaws can be given as an indention load (as in the experiments here) or by impression size or crack length (and thus might be amenable to non-destructive evaluation). The characteristic scale of the intrinsic flaws shown by the vertical dotted line conveniently separates the intrinsic strength dominated by manufacturing flaws left of the dotted line and indentation strength dominated by contact flaws right of the dotted line—these strengths are also indicated by the horizontal and diagonal asymptotes of the solid-line prediction. The intrinsic strengths to the left of the plot indicate the strongest a component can be under the given loading time conditions. The ultimate high strength is given by the inert intrinsic strength between the upper dashed lines in the upper left of the plot. As time increases, the failure stress decreases. Any points to the right of these levels indicate a decrease in strength by a more potent contact flaw. The extent of extrapolation is noted by the separation of the reference data and the reliability prediction; of course, this extent should be minimized to minimize uncertainty, but if necessary limited confirmatory tests can be made (e.g., single indentation loads, or, as here, a check on the measured intrinsic strength against the prediction, Figure 1). Although there are well-stated issues[1] with fracture reliability predictions, the scheme presented here provides a simple starting point for many ceramics.

ORCID


Robert F. Cook http://orcid.org/0000-0003-0422-8881

REFERENCES

1. Cook RF. Multi-scale effects in the strength of ceramics. *J Am Ceram Soc*. 2015;98:2933-2947.
2. Cook RF. Strength of brittle materials in moderately corrosive environments. *J Am Ceram Soc*. 2018;101:1684-1695.
3. Cook RF, Pharr GM. Direct observation and analysis of indentation cracking in glasses and ceramics. *J Am Ceram Soc*. 1990;73:787-817.
4. Cook RF. Toughening of a cordierite glass-ceramic by compressive surface layers. *J Am Ceram Soc*. 2005;88:2798-2808.
5. Liniger EG, Cook RF. A controlled flaw technique for lifetime characterization. *J Am Ceram Soc*. 1993;76:2123-2126.
6. Fuller ER Jr, Lawn BR, Cook RF. Theory of fatigue for brittle flaws originating from residual stress concentrations. *J Am Ceram Soc*. 1983;66:314-321.
7. Chantikul P, Lawn BR, Marshall DB. Micromechanics of flaw growth in static fatigue: influence of residual contact stresses. *J Am Ceram Soc*. 1981;64:322-325.
8. Wiederhorn SM, Fuller ER Jr, Mandel J, Evans AG. An error analysis of failure prediction techniques derived from fracture mechanics. *J Am Ceram Soc*. 1976;59:403-411.
9. Ritter JE Jr, Meisel JA. Strength and failure predictions for glass and ceramics. *J Am Ceram Soc*. 1976;59:478-481.
10. Jakus K, Coyne DC, Ritter JE Jr. Analysis of fatigue data for lifetime predictions for ceramic materials. *J Mater Sci*. 1978;13:2071-2080.
11. Matthewson MJ, Kurkjian CR. Environmental effects on the static fatigue of silica optical fiber. *J Am Ceram Soc*. 1988;71:177-183.
12. Roark RJ, Young WC. *Formulas for Stress and Strain*, 5th edn. Tokyo, Japan: McGraw-Hill; 1983.

How to cite this article: Cook RF. A simple method of short-term mechanical reliability prediction for ceramics in reactive environments. *J Am Ceram Soc*. 2018;101:2727–2731. https://doi.org/10.1111/jace.15526